Interaction of supercooled droplets and nonspherical ice crystals with a solid body in a mixed cloud

Ivan A. Amelyushkin
Affiliation Central Aerohydrodynamic Institute, Moscow Institute of Physics and Technology
Function Senior researcher, lecturer
Address Russia, Moscow region, Zhukovsky, Zhukovskogo street, 1, Gagarina street 16
E-mail Amelyushkin_Ivan@mail.ru

Albert L. Stasenko
Affiliation Central Aerohydrodynamic Institute, Moscow Institute of Physics and Technology
Function Principal researcher, professor
Address Russia, Moscow region, Zhukovsky, Zhukovskogo street, 1, Gagarina street 16
E-mail Stasenko@serpantin.ru

ABSTRACT

Mathematical models of nonspherical particles' motion in nonuniform flow were proposed for continuous flow approach as well as for single particles' motion simulation. Lagrangian approach was used to simulate aerosol flow with nonspherical particles around transversal cylinder. Peculiarities of supercooled water crystallization were investigated via cryostat, infrared spectroscopy and original devices for supercooled droplets' impact simulation. The results of the experimental study of the supercooled water crystallization are presented. The relationship between the parameters of intermolecular interaction with the parameters of macroscopic phenomena accompanying the crystallization of supercooled water was determined. Mathematical models of the supercooled liquid crystallization and the expression for the minimum rate for the beginning of the supercooled droplets crystallization on impact with the surface of the aircraft were developed. The numerical and experimental evaluations of physical parameters characterizing the supercooled liquid crystallization in the icing problem are performed. Two-phase boundary layer formation near nanostructutred surface was investigated via molecular dynamics method.

KEYWORDS: *nonspherical particles, supercooled droplets, aerosol flow, interaction of two-phase flow with a solid body.*

NOMENCLATURE

Latin
Re - Reynolds number
M - Mach number
$\boldsymbol{F}$ - force vector
S - scattering coefficient
q - flux
$\boldsymbol{e}$ - unity vector
e – specific energy
a - volumetrically equivalent radius
$\boldsymbol{V}$ - velocity vector
V - velocity module
$\hat{\boldsymbol{P}}$ - tensor of viscous tention
$\hat{\boldsymbol{S}}$ - strain rate tensor
$\hat{\boldsymbol{E}}$ - unity matrix
d – coefficient in linear tensor equation
u - x velocity component
v - y velocity component
f - force coefficients
E - shape parameter
R - circumfluent body's radius
m - mass
W - energy
t - time
N - number of molecules
k - constant
T - temperature
L - specific heat
r - distance between molecules or atoms
C - specific heat capacity
Nu - Nusselt number

Pr - Prandtl number
S - area
e - electron
E - energy
U - potential
c - light velocity
b - Bohr radius
$\hbar$ - Plank constant
Q - charge
Ak - spreading coefficient

Greek

φ,θ,ψ - angles of particles' orientations
δF - roof-mean-square force deviation
δ – delta function
ρ - density
ε_0 - electrical constant
μ - dynamic gas viscocity
τ - characteristic time
ξ - random number between 0 and 1
Ξ - random unity vector
Γ - friction coefficient
α - fraction, angle of attack
β - front crystallization velocity coefficient
ς - ice crystals coefficient
λ - heat transfer coefficient
Ψ - wave function
ε - Lennard-Jones energy rate
σ - Lennard-Jones distance rate

Superscripts

V - volumetric
0 - initial
Sk - Stokes
NS - nonspherical
∞ - far away from the circumfluent body
* - critical

Subscripts

p - particle
A - aerodynamic
|| - parallel
⊥ - perpendicular
x - x component
y - y component
Sk - Stokes
∞ - far away from the circumfluent body
a_p - particle's radius
l - liquid
s - solid
D - drag
1 - one molecule
k - number of stohastics' type
B – Boltsman
Br - Brownian
NS - nonspherical
Turb - turbulent
Det - deterministic
R - relaxation
0 - initial
F - flow
f - freezing
b - barrier
m - mass
e - electron
i - number of atom or electron
j - number of atom
H - hydrogen
O - oxygen
w-H_2O - between wall and H_2O
H_2O-H_2O - between H_2O and H_2O

1 INTRODUCTION

Multiphase flows are widespread in nature and human practice. Aircraft safety and ice accretion simulation are important problems in aeronautical sciences[1–5]. Present paper concerns nonspherical particles[6,7] and supercooled droplets[3,4] with application for aircraft icing investigations. Flight in mixed (droplets/crystals) clouds is accompanied by many physical processes – trajectory bounding of solid or liquid particles, their impingement upon a surface, bouncing or damage, mutual collisions, etc. A multitude of investigations (both theoretical and experimental) has been devoted to these phenomena almost from almost the beginning of aviation history(e.g. [2]), but the problem of anti and deicing is far from its final solution due to complex inter-relations of between the abovementioned physical processes[5,8]. The paper presented tends to reveal some their intrinsic features.

The role of water crystals orientation is investigated in nonsymmetrical impingement upon transversal cylinder. The correspondent numerical analysis was developed for small Reynolds numbers (especially in microaviation application) as well as for large those, on the basis of the spheroid model of crystal.

The qualification characteristics of supercooled drops ice crystal-air flow (especially, radial distribution of the particulate concentration) are investigated and developed theoretically [1, 3] and experimentally [3, 4]. In previous publications original algorithms were proposed to determine two phase flow parameters in wind tunnels via laser sheet images analysis [9], optical system for aerosol flow with ice crystal and supercooled droplets' was developed as well as corresponding methods of flow visualization and image processing[9]. Peculiarities of supercooled droplets and nonspherical ice

crystal interaction with a solid body were investigated via molecular dynamics and Lagrangian mechanics technique.

2 MATHEMATICAL SIMULATION OF NONSPHERICAL PARTICLES' MOTION

2.1 Theoretical calculation of nonspherical particles' scattering coefficient

In spite of a lot of different mathematical models for aerohydrodynamic characteristics of single nonspherical particles'[8,10–13], simulation of the whole two-phase flow with nonspherical particles becomes problematic [6,7]. In order to calculate scattering coefficient of nonspherical particles and orientational force let us calculate an average force, which acts on a particle. It may be calculated from the following expression:

$$< \boldsymbol{F}(\mathrm{Re},\mathrm{M}) >= \boldsymbol{F}_{\mathrm{A}} = \frac{\int\int\int \boldsymbol{F}(\mathrm{Re},\mathrm{M},\varphi,\theta,\psi)\mathrm{d}\varphi\mathrm{d}\theta\mathrm{d}\psi}{\int\int\int \mathrm{d}\varphi\mathrm{d}\theta\mathrm{d}\psi}$$

The expression for the roof-mean-square deviation from this average force is

$$\delta F_{\mathrm{NS}}(\mathrm{Re},\mathrm{M}) = \sqrt{\frac{\int_0^{2\pi}\int_0^{2\pi}\int_0^{2\pi} \left|\boldsymbol{F}(\mathrm{Re},\mathrm{M},\varphi,\theta,\psi) - \boldsymbol{F}_{\mathrm{A}}(\mathrm{Re},\mathrm{M})\right|^2 \mathrm{d}\varphi\mathrm{d}\theta\mathrm{d}\psi}{\int_0^{2\pi}\int_0^{2\pi}\int_0^{2\pi} \mathrm{d}\varphi\mathrm{d}\theta\mathrm{d}\psi}} = \sqrt{\int_0^{2\pi}\int_0^{2\pi}\int_0^{2\pi} \left|\boldsymbol{F}(\mathrm{Re},\mathrm{M},\varphi,\theta,\psi) - \boldsymbol{F}_{\mathrm{A}}(\mathrm{Re},\mathrm{M})\right|^2 \mathrm{d}\varphi\mathrm{d}\theta\mathrm{d}\psi} \Big/ \sqrt{4\pi^3}$$

Expression for scattering coefficient of nonspherical particles is introduced as follows: $S_{\mathrm{NS}} = \sqrt{\frac{\delta F_{\mathrm{NS}}}{\rho_0}}$, [m^2/s].

Scattering of particles leads to the appearance the additional mass flow rate: $\boldsymbol{q}_m^{\mathrm{NS}} = S_{\mathrm{NS}}(\rho_p^V + \rho)\overline{\nabla}\left(\frac{\rho_p^V}{\rho_p^V+\rho}\right) \rightarrow S_{\mathrm{NS}}\overline{\nabla}\rho_p^V$, which takes place in the governing equations[6] for two-phase flow motion.

Neglecting phase transitions and collisions between particles equations aerosol flow motion will be following ones[2]:

1. Mass conservation equations:

$\frac{\partial \rho_p^V}{\partial t} + \left(\overline{\nabla}\cdot\rho_p^V\boldsymbol{V}_p\right) = \boldsymbol{q}_m^{\mathrm{NS}}$ – for nonspherical particles' mass concentration ρ_p^V.

Here $\boldsymbol{V}_p$ – vector of particles' velocity, t – time.

$\frac{\partial \rho}{\partial t} + \left(\overline{\nabla}\cdot\rho\boldsymbol{V}\right) = -\boldsymbol{q}_m^{\mathrm{NS}}$ – for gas density ρ, here $\boldsymbol{V}$ – gas velocity.

2. Momentum conservation equations:

$\rho_p^V \frac{\mathrm{d}\boldsymbol{V}_p}{\mathrm{d}t} = \frac{\rho_p^V}{m_p}\boldsymbol{F}_p + \overline{\nabla}\boldsymbol{q}_m^{\mathrm{NS}}\boldsymbol{V}_p$ – for particles; $\rho\frac{\mathrm{d}\boldsymbol{V}}{\mathrm{d}t} = \overline{\nabla}\cdot\hat{\boldsymbol{P}} - \frac{\rho_p^V}{m_p}\boldsymbol{F}_p - \overline{\nabla}\boldsymbol{q}_{\boldsymbol{m}}^{\mathrm{NS}}\cdot\boldsymbol{V}$ – for gas.

Here $m_p = \frac{4}{3}\pi a_p^3\rho_p$ – mass of a single volumetrically equivalent particle, where a_p – is a radius of a sphere whose volume equals a volume of nonspherical particle, $\boldsymbol{F}_p$ – force, which acts on particles from gas. Various kinds of mathematical models for this force are given in [10–13]. According to simple physical estimations and numerical calculations for particle's motion in a gas, the dominant force is drag force $\boldsymbol{F}_p = \frac{\pi a_p^2\rho}{2}C_D\left|\boldsymbol{V}-\boldsymbol{V}_p\right|\left(\boldsymbol{V}-\boldsymbol{V}_p\right)$, C_D – drag coefficient. The first component in the right side of pulse equation for gas is viscous strain tensor: $\hat{\boldsymbol{P}} = 2\mu\hat{\boldsymbol{S}} + d\hat{\boldsymbol{E}}$, where $\hat{\boldsymbol{S}}$ strain tensor rate:, $\hat{\boldsymbol{E}}$ – unity matrix, μ –dynamic gas viscosity, $d = -P - \left(\frac{2\mu}{3} - \frac{\zeta}{3}\right)\overline{\nabla}\cdot\boldsymbol{V}$, P – gas pressure, ζ – volume viscosity.

3. Energy balance equations:

$\rho_p^V \frac{de_p}{dt} = \frac{\rho_p^V}{m_p} \boldsymbol{F}_p \cdot \boldsymbol{V}_p + \overline{\nabla} \boldsymbol{q}_m^{NS} \frac{\boldsymbol{V}_p^2}{2} + \frac{\rho_p^V}{m_p} Q_p$ – for energy density of nonspherical particles:

$e_p = U_0 + C_0 T_p + \frac{|\boldsymbol{V}_p|^2}{2}$;

$\rho \frac{de}{dt} = \overline{\nabla} \hat{\boldsymbol{P}} \cdot \boldsymbol{V} - \overline{\nabla} \boldsymbol{q}_m^{NS} \frac{\boldsymbol{V}^2}{2} + \overline{\nabla}(\lambda \overline{\nabla} T) - \frac{\rho_p^V}{m_p} \boldsymbol{F}_p \cdot \boldsymbol{V}_p - \frac{\rho_p^V}{m_p} Q_p$ – for gas energy density $e = \frac{C_V}{\mu_m} T_p + \frac{|\boldsymbol{V}_p|^2}{2}$.

U_0 – internal energy of particles, C_0 – specific heat capacity of particles' material, λ – is a gas heat conductivity coefficient, T_p – temperature of particles, T – gas temperature. $Q_p = 2\pi a_p \lambda (T_p - T) \mathrm{Nu}(\mathrm{Re}, \mathrm{Pr})$ – heat flux from gas to moving particles, where

$\mathrm{Nu} = 2 + \frac{1}{2} \mathrm{Re}_p^{\frac{1}{2}} \mathrm{Pr}^{\frac{1}{3}}$ – Nusselt number for turbulent circumvallation of volumetrically equivalent particle, $\mathrm{Re} = 2a_p \rho |\boldsymbol{V} - \boldsymbol{V}_p| / \mu$, $\mathrm{Pr} = \mu C_p / \mu_m \lambda$ – Prandl number.

A described above system of equations could be used for simulation two phase flows with nonspherical particles or ice crystals.

Let us describe the particle orientation via unity vector which is directed along major semiaxis $\boldsymbol{e}_{\|} = \boldsymbol{e}_x \cos\theta - \boldsymbol{e}_y \sin\theta$. Velocity components of it's motion relative to the carrying gas are: $\boldsymbol{V} - \boldsymbol{V}_p = \Delta \boldsymbol{V} = \boldsymbol{e}_x (u - u_p) + \boldsymbol{e}_y (v - v_p)$. It's components in a reference frame, which is connected with a particle equal

$|\boldsymbol{V} - \boldsymbol{V}_p|_{\|} = |\boldsymbol{V} - \boldsymbol{V}_p| \cos\alpha$, $|\boldsymbol{V} - \boldsymbol{V}_p|_{\perp} = |\boldsymbol{V} - \boldsymbol{V}_p| \sin\alpha$, where

$\cos\alpha = \frac{(\boldsymbol{V} - \boldsymbol{V}_p)\boldsymbol{e}_{\|}}{|\boldsymbol{V} - \boldsymbol{V}_p||1|} = \frac{(u - u_p)\cos\theta - (v - v_p)\sin\theta}{\sqrt{(u - u_p)^2 + (v - v_p)^2}}$, $\sin\alpha = \frac{(\boldsymbol{V} - \boldsymbol{V}_p)\boldsymbol{e}_{\|}}{|\boldsymbol{V} - \boldsymbol{V}_p||1|} = \frac{(u - u_p)\sin\theta + (v - v_p)\cos\theta}{\sqrt{(u - u_p)^2 + (v - v_p)^2}}$.

Angles, which are used in equations are shown in Fig. 1.

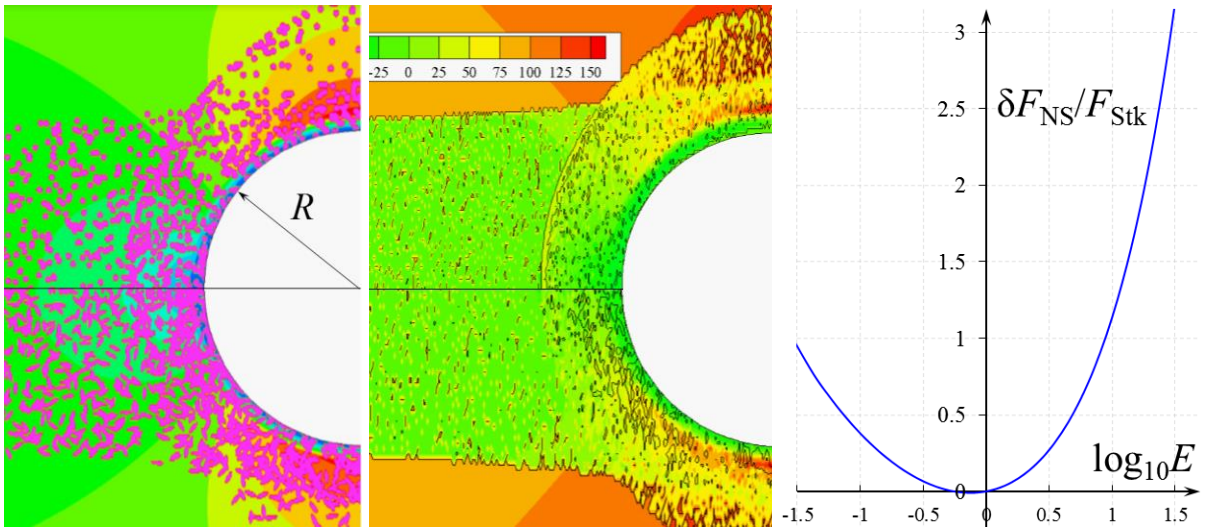

Figure 1: Comparison of flows with spherical and nonspherical particles near a solid body: on the left – particles' locations; in the center – comparison of velocity nonequilibrium of the corresponding flows distribution; at right – dependence of orientation force on the shape parameter *E*

For small Reynolds numbers, we used the following expression for force, which acts on the ellipsoidal particle:

$$\boldsymbol{F} = 6\pi\mu a_p \left[f_{\|} (\boldsymbol{V} - \boldsymbol{V}_p)_{\|} + f_{\perp} (\boldsymbol{V} - \boldsymbol{V}_p)_{\perp} \right] \quad (1)$$

$$\boldsymbol{F}(\mathrm{Re},\mathrm{M}) \cong \boldsymbol{F}(\mathrm{Re}) = \frac{\rho\pi a_p^2}{2}\frac{24}{\mathrm{Re}_p}\left|\boldsymbol{V}-\boldsymbol{V}_p\right|\left[f_{\parallel}\left(\boldsymbol{V}-\boldsymbol{V}_p\right)_{\parallel} + f_{\perp}\left(\boldsymbol{V}-\boldsymbol{V}_p\right)_{\perp}\right] = 3\pi\frac{\mu^2}{\rho}\mathrm{Re}_p\left[f_{\parallel}\cos\theta\boldsymbol{i}_{\parallel} + f_{\perp}\sin\theta\boldsymbol{i}_{\perp}\right]$$

$$< \boldsymbol{F}(\mathrm{Re},\mathrm{M}) >=< \boldsymbol{F}(\mathrm{Re}) >= \boldsymbol{F}_{\mathrm{A}} = 6\pi\mu a_p\sqrt{\int\int\int\left[\left(f_{\parallel}\left(\boldsymbol{V}-\boldsymbol{V}_p\right)_{\parallel}\right)^2 + \left(f_{\perp}\left(\boldsymbol{V}-\boldsymbol{V}_p\right)_{\perp}\right)^2\right]\mathrm{d}\varphi\mathrm{d}\theta\mathrm{d}\psi \Big/ \int\int\int\mathrm{d}\varphi\mathrm{d}\theta\mathrm{d}\psi} =$$

$$= 3\pi\frac{\mu^2}{\rho}\mathrm{Re}_p\sqrt{\frac{f_{\parallel}^2 + f_{\perp}^2}{2}}$$

Here $\boldsymbol{V}-\boldsymbol{V}_p = \left(u-u_p\right)\boldsymbol{e}_x + \left(v-v_p\right)\boldsymbol{e}_y$; $f_{\parallel}$ and $f_{\perp}$ – coefficients for force which acts on nonspherical particle.

For three-dimensional case, components of particle's relative to the gas motion are:

$$\left(\boldsymbol{V}-\boldsymbol{V}_p\right)_{\parallel} = \left(u-u_p\right)\cos\varphi\sin\theta = \left|\boldsymbol{V}-\boldsymbol{V}_p\right|\cos\varphi\sin\theta; \qquad \left(\boldsymbol{V}-\boldsymbol{V}_p\right)_{\perp} = \left(u-u_p\right)\sin\varphi = \left|\boldsymbol{V}-\boldsymbol{V}_p\right|\sin\varphi;$$

$$< \boldsymbol{F}(\mathrm{Re}) >= \boldsymbol{F}_{\mathrm{A}} = \frac{\int\int\int 6\pi\mu a_p\left[f_{\parallel}\left(\boldsymbol{V}-\boldsymbol{V}_p\right)_{\parallel} + f_{\perp}\left(\boldsymbol{V}-\boldsymbol{V}_p\right)_{\perp}\right]\mathrm{d}\varphi\mathrm{d}\theta\mathrm{d}\psi}{\int\int\int\mathrm{d}\varphi\mathrm{d}\theta\mathrm{d}\psi} = 6f_{\perp}\frac{\mu^2}{\rho}\mathrm{Re}_p \cong \frac{6}{5}\frac{\mu^2}{\rho}\frac{3+2E}{E^{1/3}}\mathrm{Re}_p;$$

$$\delta F_{\mathrm{NS}}^2 = \frac{\int\int\int\left(\boldsymbol{F}(\mathrm{Re},\mathrm{M},\varphi,\theta,\psi)-\boldsymbol{F}_{\mathrm{A}}\right)^2\mathrm{d}\varphi\mathrm{d}\theta\mathrm{d}\psi}{\int\int\int\mathrm{d}\varphi\mathrm{d}\theta\mathrm{d}\psi} = \left(\frac{3\mathrm{Re}_p\mu^2}{\rho\pi}\right)^2\left[f_{\parallel}^2\frac{1}{4} + \left(\frac{8-15\pi^2}{2\pi^2}\right)f_{\perp}^2\right]$$

So the ratio between orientational force and Stokes force depends on shape parameter as follows:

$$\frac{\delta\boldsymbol{F}(\mathrm{Re})}{\boldsymbol{F}_{\mathrm{Sk}}(\mathrm{Re})} = \left|1-\frac{<\boldsymbol{F}(\mathrm{Re})>}{\boldsymbol{F}_{\mathrm{Sk}}(\mathrm{Re})}\right| = \left|1-\sqrt{\frac{f_{\parallel}^2+f_{\perp}^2}{2}}\right| \cong \left|1-\frac{1}{E^{1/3}}\sqrt{\frac{E^2+4E+5}{10}}\right|$$

For values' gap ¼ < E < 4 one has the following approximate expressions for force components: $f_{\parallel} = \left(\frac{4}{5}+\frac{E}{5}\right)\frac{1}{E^{1/3}}$, $f_{\perp} = \left(\frac{3}{5}+\frac{2E}{5}\right)\frac{1}{E^{1/3}}$.

The above described model for small Reynolds numbers could be developed for higher Reynolds numbers as follows: $F^{NS} = F_{Sk}^{NS}\frac{C_D(Re,M)}{c_D^{Sk}} = \boldsymbol{F}_{Sk}^{NS}\frac{C_D(Re,M)}{24/Re_p}$

"Fig. 1" illustrates the difference between spherical and nonspherical particles' behavior. Calculations were carried out with the following flow parameters: R=12.5·10^{-3} m, a_p = 10^{-6} m, ρ_p=917 kg/m^3(ice crystal), V_∞ = 6 m/s, T_∞ = 273 K, P_∞ = 10^5 Pa, μ_∞≈1.7·10^{-5} Pa·s, Re_∞≅3, Re_p^∞=2.4·10^{-3}<<1. Assumptions of characteristic times (flow time $\tau_F = R/V_\infty$≈2·10^{-3} s; particles' relaxation time $\tau_R = \frac{2}{9}\frac{a_p^2\rho_p}{\mu}$ ≅1.2·10^{-3} s; $\tau_{a_p} = \frac{a_p}{V_\infty}$≈2·10^{-8} s << τ_R < τ_F) allows to neglect nonstationary effects and to use formula (1).

The developed mathematical models (as well as corresponding numerical algorithms) could be applied for space debris simulation and prediction of its behavior.

2.2 Numerical algorithm for particles' stochastic motion calculation

The first way to describe stochastic motion is to use additional accelerations for particles which equals $\boldsymbol{\Xi}\delta\boldsymbol{F}\cdot\xi$. Here ξ – is a random number which takes values uniformly distributed from 0 to 1, $\boldsymbol{\Xi}$ – random unity vector. Thus equation for stochastic particle's motion will be the following:

$$m_p\frac{\mathrm{d}\boldsymbol{V}_p}{\mathrm{d}t} = \sum\boldsymbol{F}_{\mathrm{Det}} - \Gamma\boldsymbol{V}_p + \delta(t)\sum_{k=1}^{k_{\max}}\boldsymbol{\Xi}_k\delta F_k\cdot\xi_k \qquad (2)$$

The sum is taken for all type of stochastic mechanisms. For aerosol, the most significant sources of particles' stochastics are: 1. turbulent flow pulsations; 2. nonspherical shape of particles; 3. Brownian motion of small particles and surrounding molecules. For each type of stochastics pseudodiffusion (or

scattering) coefficients are calculated and used in formula (2). This equation describes more general processes in comparison Brownian dynamics [14].

Another way to calculate stochastic motion of particles is to use characteristic velocities for each particle's motion: $\mathbf{V}_p = \mathbf{V}_p^0 + \frac{|\mathbf{V}'|}{\sqrt{1+t/\tau_R}} \cdot \mathbf{\Xi}_{\mathbf{Turb}} + \sqrt{\frac{8k_B T}{\pi m_1 N}} \cdot \mathbf{\Xi}_{\mathbf{Br}} + V_{NS} \cdot \mathbf{\Xi}_{\mathbf{NS}}$

Orientational force δF_{NS} which acts on particle could be described by the following equation:

$$\delta \boldsymbol{F}(\mathrm{Re}) = 3\pi \frac{\mu^2}{\rho} \mathrm{Re}_p \left| 1 - \frac{1}{E^{1/3}} \sqrt{\frac{E^2+4E+5}{10}} \right|$$

Friction coefficient is defined from analysis of physical quantities' dimensions:

$$S_{NS} \sim V_{NS} L_{NS}; \qquad \delta F_{NS} L_{NS} = \delta F_{NS} \frac{S_{NS}}{V_{NS}} \sim \frac{m_p V_{NS}^2}{2};$$

So one can obtain expression for friction coefficient:

$$\Gamma_{NS} \sim \frac{\delta F_{NS}}{V_{NS}} = \delta F_{NS} \left(\frac{m_p}{\delta F_{NS} S_{NS}} \right)^{1/3} = \delta F_{NS} \left(\frac{m_p}{\delta F_{NS} \sqrt{\delta F_{NS}/\rho_0}} \right)^{1/3}.$$

And equation for nonspherical particles' stochastic and deterministic motion will be as follows:

$$m_p \frac{d\boldsymbol{V}_p}{dt} = \sum \boldsymbol{F}_{\mathbf{Det}} - \Gamma_{NS} \boldsymbol{V}_p + \delta(t) \mathbf{\Xi}_{NS} \delta F_{NS} \cdot \xi_{NS}.$$

Table 1 illustrate basic characteristic parameters of nonspherical particles's chaos (or "gas").

Table 1: Parameters of nonspherical particles' chaos

Physical quantity	Letter	Formula	Dimension
Orientational force	δF_{NS}	$\left\|1-\sqrt{\frac{f_\parallel^2+f_\perp^2}{2}}\right\| 6\pi a\mu V = \left\|1-\sqrt{\frac{f_\parallel^2+f_\perp^2}{2}}\right\| 3\pi \frac{\mu^2}{\rho} \mathrm{Re}_p$	N
Scattering coefficient	S_{NS}	$\sqrt{\frac{\delta F_{NS}}{\rho_0}} = \frac{\mu}{\sqrt{\rho\rho_0}} \sqrt{\left\|1-\sqrt{\frac{f_\parallel^2+f_\perp^2}{2}}\right\| 3\pi \mathrm{Re}_p}$	m^2/s
Velocity	V_{NS}	$\left(\frac{\delta F_{NS} \sqrt{\delta F_{NS}/\rho_0}}{m_p} \right)^{1/3}$	m/s
Length	L_{NS}	$S_{NS} \left(\frac{m_p}{\delta F_{NS} S} \right)^{1/3} = \sqrt{\frac{\delta F_{NS}}{\rho_0}} \left(\frac{m_p}{\delta F_{NS} \sqrt{\delta F_{NS}/\rho_0}} \right)^{1/3}$	m
Time	τ_{NS}	$\sqrt{\frac{\delta F_{NS}}{\rho_0}} \left(\frac{m_p}{\delta F_{NS} \sqrt{\delta F_{NS}/\rho_0}} \right)^{2/3} = \frac{m_p^{2/3}}{\sqrt{\rho_0^{1/3} \delta F_{NS}}}$	s
Friction coefficient	Γ_{NS}	$\delta F_{NS} \left(\frac{m_p}{\delta F_{NS} \sqrt{\delta F_{NS}/\rho_0}} \right)^{1/3}$	$kg(m/s)^3$
Pressure	P_{NS}	$\rho_p^V \delta V_{NS}^2 = \rho_p^V \left(\delta F_{NS} \sqrt{\delta F_{NS}/\rho_0}/m_p \right)^{2/3} = \rho_p^V \delta F_{NS} \left(\rho_0 m_p^2 \right)^{-1/3}$	Pa

3 PECULIARITIES OF SUPERCOOLED WATER CRYSTALLIZATION

Physical mechanism of supercooled water crystallization plays important role in aircraft icing control and development of methods of mathematical and numerical simulation [1, 2, 4, 8].

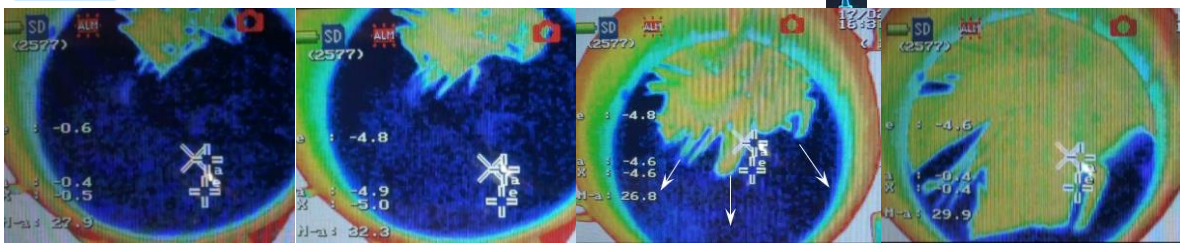

Figure 2: Infrared spectroscopy of crystallization front propagation

In "Fig 2" and "Fig 3" one may see our recent results of investigations of water freezing peculiarities according to the experimental data and some results of previous world experiences. Initial temperature of supercooled distillate water is approximate – 4 ° C, ambient temperature is approximately 15 ° C. Crystallization process was initiated with and ice crystal dropped in the water surface.

"Fig. 2" shows infrared spectroscopy visualization of supercooled water crystallization front propagation. One can see a complex nonuniform structure of crystallization front.

We carried out experiments of supercooled water interaction with a solid body and determined the expression for specific energy barrier $L_b(T)$ dependence on supercooled temperature T. According to approximation experimental data ("Fig. 3") we obtained the following expression:

$$L_b(T) = L_b^0\left(1 - T/T_f\right)^{-7/5}, \tag{3}$$

where $L_b^0 \cong 4\cdot 10^{-3}$ J/kg. Tendency of L_b to infinity at $T = T_f$ could be explained via the fact, that at this temperature water does not crystallizes even when mechanical impact are significant. The correspondent expression for critical velocity of droplet impingement dependence on temperature is

$$V^*(T) = V_0^*\left(1 - T/T_f\right)^{-7/10}, \tag{4}$$

where $V_0^* \cong 8.9\cdot 10^{-2}$ m/s. This expression could be used for aircraft icing calculations in order to determine conditions when supercooled droplets crystallize. According to experiments and previous publications[15–17] dependence of supercooled water front crystallization is as follows:

$$V = \beta(T_f - T)^2, \tag{5}$$

where $\beta = (3.75 \pm 0.4)\cdot 10^{-3}$ m/s·K^2 – coefficient which is determined from experimental results. This expression could also be rewritten as follows:

$$V/V_0 = \left(1 - T/T_f\right)^2, \tag{6}$$

where $V_0 = \beta T_f^2 = 280 \pm 30$ m/s – characteristic velocity.

It should be noted that after front crystallization propagation water liquid transforms into suspension of liquid water and ice crystals [15, 17]. According to our experimental investigations ("Fig. 2") ice mass fraction in a liquid water after front crystallization propagation is described by the following equation:

$$\alpha_m(T) \cong \varsigma\sqrt{1 - \frac{T}{T_f}}, \tag{7}$$

where $\varsigma = (2 \pm 0.5)$ °K$^{-1/2}$. After crystallization, front propagation far away from the circumfluent body droplet will not transform into ice before impact on a body surface. The following estimation shows the comparison characteristic times of crystallization and characteristic time of the flow $\frac{\tau}{\tau_{flow}} \cong \frac{V_\infty L(1-\alpha_m)a_p^2\rho_p}{R3\lambda(T_f - T)} = 1850\left(1 - 0.12\sqrt{\Delta T}\right)/\Delta T \sim 10^1 - 10^3 >> 1.$ This estimation was made from the following equation:

$$L\frac{\Delta m}{\tau} = L(1-\alpha_m)\frac{4}{3}\pi a_p^3\rho\tau^{-1} \cong Q = \mathrm{Nu}2\pi a_p\lambda(T_f - T) = 2\pi a_p\lambda(T_f - T)\left(2 + \frac{1}{2}\mathrm{Re}^{\frac{1}{2}}\mathrm{Pr}^{\frac{1}{3}}\right).$$

Here a_p – radius of the particle (droplet). Because of small Reynolds number Re which is based on the difference between particle's and gas velocities, the freezing time is $\tau \cong \frac{L(1-\alpha_m)a_p^2\rho_p}{3\lambda(T_f - T)}$. For

estimations we used following parameters: droplet density ρ_p = 10^3 kg/m^3, water heat transfer coefficient λ = 0.6 W/m·K, specific heat of crystallization L = 0.33 MJ/kg, flow velocity V_∞ = 100 m/s, characteristic size of a circumfluent body 0.1 m.

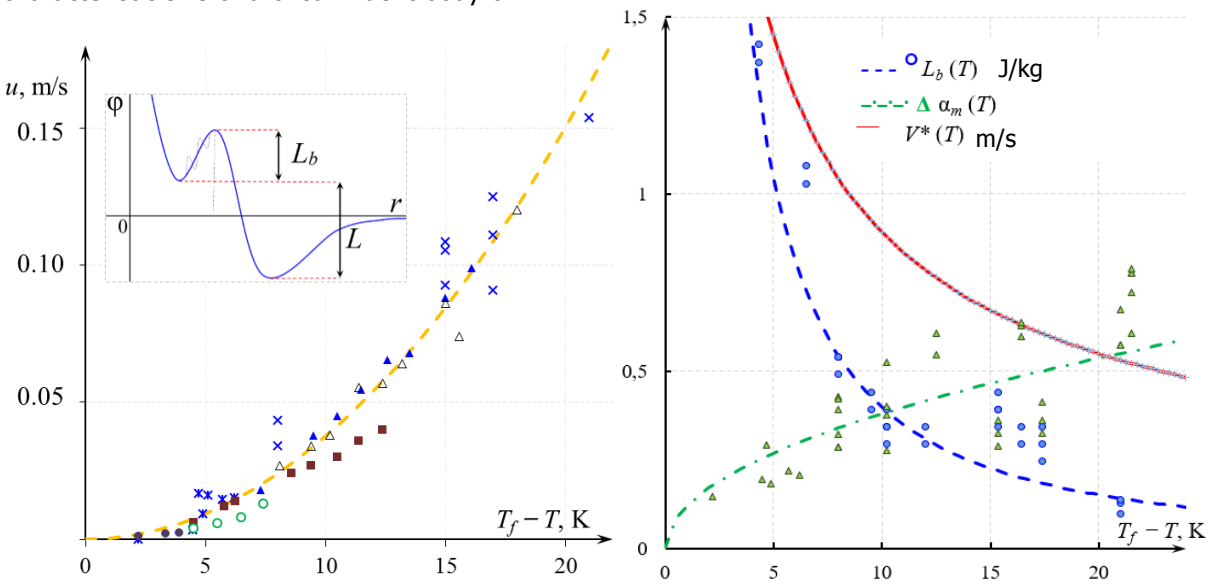

Figure 3: On the left – dependence of supercooled water crystallization front velocity on temperature: crosses data of present article's authors; markers – experimental data from [17], dashed curve – parabolic interpolation. A small plot above on the left shows qualitative dependence of liquid pair interaction potential on intermolecular distance; On the right – dependence of specific energy barrier L_b of supercooled metastable water on temperature T: circles – experimental data, blue dashed curve – their approximation; triangles – experimental results of ice mass fraction α_m after propagation of crystallization front, dot and dash-dotted curve – its approximation, continuous curve shows the dependence of critical velocity of suddenly shattered liquid on solid body surface on temperature

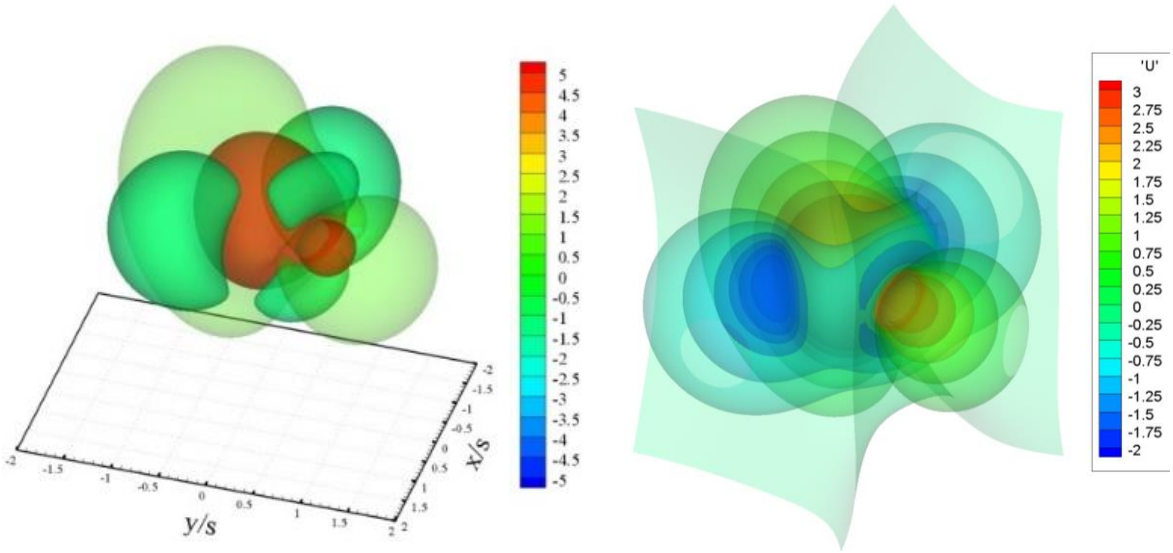

Figure 4: Equipotential surfaces of TIP4P water pair interaction potential

"Fig. 4" shows that the water molecules pair interaction potential is significantly nonsymmetrical. One can see semitransparent equiscalar surfaces of this potential. Values of these isosurfaces are related to the characteristic value ε_{H_2O}=1.12·10^{-20} J. For this example, we used water molecules pair interaction potential TIP4P [18]: $U(r_1,r_2) = 4\varepsilon\left[\left(\frac{\sigma}{r_{12}}\right)^{12} - \left(\frac{\sigma}{r_{12}}\right)^{6}\right] + \sum_i \sum_j \frac{Q_i Q_j}{4\pi\varepsilon_0 r_{ij}}$, here R_1, R_2 –radius-vectors of two molecules' mass centers, r_{ij} – radius-vectors between water charged atoms, ε_0 – galvanometric constant, σ=3.154·10^{-10} m, ε=1.0772·10^{-21} J, Q_H=0.52 e, Q_O=–1.04 e, e – charge of

the electron. The presence of potential wells in intermolecular interaction potential explains peculiarities of supercooled water crystallization.

It should be noted that crystallization may be accompanied with infrared radiation [19] or electrization [20], due to the sudden change in the organization and the internal state of liquid molecules freezing, can be accounted as one of the crystallization phase heat transfer channels. Let us estimate the density of this radiation flux q when supercooled water crystallizes:

$$q\Delta S\Delta t = C\Delta m(T_f - T) - L\Delta m a_m = (C(T_f - T) - La_m)\rho\Delta SV\Delta t \quad (8)$$

from this equation one can obtain $q = \rho V\left(C(T_f - T) - L\alpha_m\right)$

Here Δm – mass element, ΔS – area element, Δt – small time interval; C – water specific heat capacity.

4 MOLECULAR DYNAMIC SIMULATION OF A SURFACE ICING

In order to simulate physical mechanism of aircraft icing and supercooled water crystallization, we used *ab initio* calculations and molecular dynamics technique[21-23]. To simulate droplets' impingement on solid body in a boundary layer, we developed numerical algorithm which is described in [24, 25]. Water molecules interact with each other via pair interaction potential. In order to determine potential of interaction between water molecule and solid body we used *ab initio* calculations.

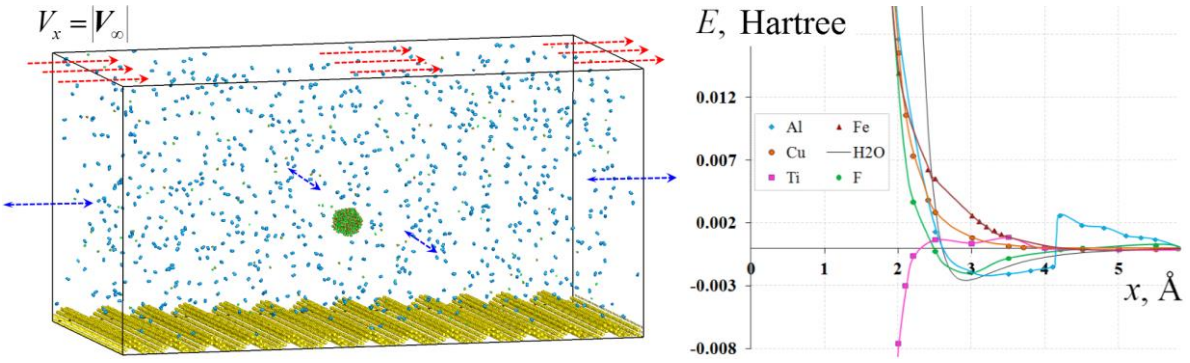

Figure 5: On the left – computation region for molecular dynamics study of water particle motion in the boundary layer of a wet air; On the right – *ab initio* calculation of potentials of interaction between water molecule with solid body atoms: 0 – water- water; 2 – water- iron; 3 – water- copper; 4 – water- titanium; 5 – water- ftourine

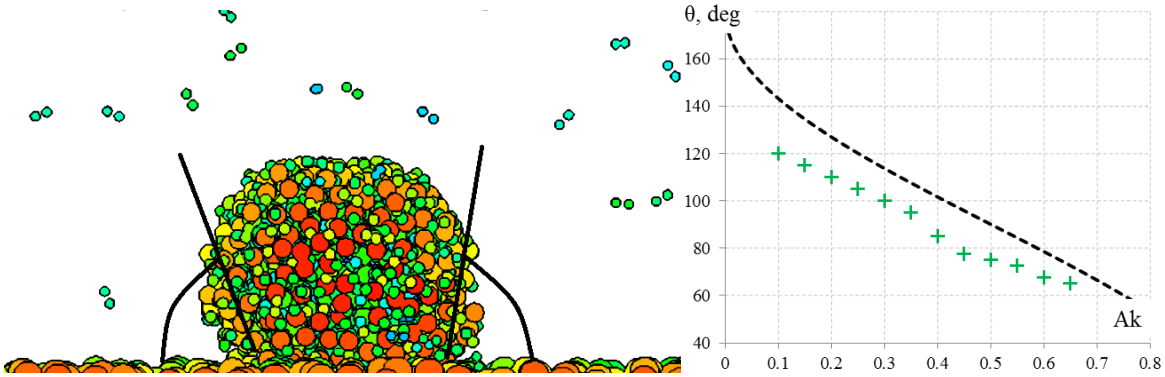

Figure 6: On the left – Illustration of water droplet behavior on a flying vehicle's surface; on the right – dependence of calculated via molecular dynamic wetting angle with corresponding angle which was obtained from expression (9)

"Fig. 5" illustrates results of quantum chemistry calculation of characteristic energy of interaction between water molecule and solid body atoms. Calculations of Schrödinger equation for multielectron atomic system were carried out in a basis: #T MP2/6-311+G(d,p):

$\sum_{i=1}^{N}\Delta_i\Psi+\frac{2m}{\hbar^2}\left(E-U+\sum_{i=1}^{N}\frac{1}{4\pi\varepsilon_0}\frac{e^2}{r_i}\right)\Psi=0$, where $=\frac{1}{2}\sum_{i=1}^{N}\sum_{k=1,k\neq i}^{N}\frac{1}{4\pi\varepsilon_0}\frac{e^2}{r_{ik}}$. Here Δ – is Laplace operator $\Delta_i=\frac{\partial^2}{\partial x_i^2}+\frac{\partial^2}{\partial y_i^2}+\frac{\partial^2}{\partial z_i^2}$.

In order to transform energy values from Hartree to Joules, one may use the following equation: $1\ \text{Hartree}=\frac{\hbar^2}{m_e b^2}=\frac{\hbar c\alpha}{b}=4.36\cdot10^{-18}\ J$.

In "Fig. 6" One can see that formula for spreading coefficient

$$\text{Ak}=\frac{\varepsilon_{W-H_2O}}{\varepsilon_{H_2O-H_2O}}\cong\frac{1+cos\theta}{2} \qquad (9)$$

coarsely approximates results of molecular dynamics calculations. Algorithms of molecular dynamic simulation of interaction between water molecules with solid body atoms was developed from previous publications[24,25].

Conclusion

Mathematical models of nonspherical particles' motion in nonuniform flow were developed. Results of numerical simulation of aerosol flow with nonspherical particles near a transversal cylinder were presented. Original mathematical models for stochastic motion of nonspherical particles were investigated. Mathematical models of peculiarities of supercooled water crystallization were developed and based on presented experimental data. In particular, the dependence of specific energy barrier of supercooled water on cooling temperature was obtained. Dependence of mass fraction of ice crystals on cooling temperature which appear after crystallization front propagation thorough metastable supercooled water was also obtained. Experimental estimation of critical impingement velocity which characterizes the beginning of metastable supercooled droplets' crystallization when they impinge the solid surface was made. Molecular dynamic study of interaction aerosol flow with a solid body showed correlation between wetting angle with spreading coefficient.

ACKNOWLEDGEMENTS

The work is supported by grant of Russian scientific foundation (project No 16–19–10472).

REFERENCES

1. Y. Bourgault, H. Beaugendre, W.G. Habashi; 2000;"Development of a shallow water icing model in FENSAP-ICE"; *AIAA Journal of Aircraft*; 37; pp. 640-646.
2. R. Böttger; 1935;"Investigation on the possibility to use disc and cone for aerodynamic drag measurement in a process of ice accretion"; *IZWB FB*; Berlin; 462, 12 pp.(in German).
3. W.D. Bachalo, C. Sipperley, G. Payne; 2011;"Aircraft icing research: challenges in cloud simulation and characterization ILASS Americas*"; 23-nd Annual Conference on Liquid Atomization and Spray Systems*; Ventura; CA.; May 2011; Disc; Paper No 3; pp. 1 - 14.
4. A.B. Miller, Yu.F. Potapov, A.L. Stasenko; 2014;"Experimental and theoretical investigation of aircraft icing in the case of crystal and mixed-phase flow"; *29th Congress of the International Council of the aeronautical sciences*; September 7th–12th 2014; St-Petersburg; Russia; 0576; pp. 1 – 6.
5. J. Hallen, G.A. Isaac; 2008;"Aircraft icing in glaciated and mixed phase clouds"; *J. Aircraft*; 45(6); pp. 2120 - 2130.
6. I.A. Amelyushkin; 2016;"Mathematical models and optical investigation of two phase flows in wind tunnels"; *Proceedings from the 30th Congress of the International Council of the Aeronautical Sciences* ICAS-2016 25th–30th September 2016; Daejeon, Korea; Paper No 2016_0665; pp. 1 -5.
7. D. Vancenzi; 2013;"Orientation of nonspherical particles in an axisymmetrical random flow"; J. *Fluid. Mech*. Cambridge Univercity Press; 719. pp. 465-487.
8. S. Nilamdeen S., W.G. Habashi; 2011;"Multiphase approach toward simulating ice crystal ingestion in jet engines"; *J. Propulsion and Power*; 27(5); pp. 959 - 969.
9. I.A. Amelysuhkin, S.E. Filippov, Yu.H. Ganiev, O.A. Gobyzov, Yu.M. Lipnitsky, Yu.A. Lozhkin; 2017;"Nonequilibrium aerosol flow in supersonic wind tunnel"; *TsAGI Science Journal*; 1(1); pp. 53 - 71.

10. S. Laín, M. Sommerfeld; 2007;"A study of the pneumatic conveying of non-spherical particles in a turbulent horizontal channel flow"; *Brazilian Journal of Chemical Engineering*; 24(04); pp. 535 – 546.
11. D. Vincenzi; 2013;"Orientation of nonspherical particles in an axisymmetric random flow"; *J. Fluid Mech.*; Cambridge University Press; 719; pp. 465 - 487.
12. G.B. Jeffery; 1922;"The motion of ellipsoidal particles immersed in a viscous fluid"; *Proc. Roy. Soc.*; A.1922; 102; pp. 161 - 179.
13. D.O. Njobuenwu, M. Fairweather; 2015;"Dynamics of single, nonspherical ellipsoidal particles in a turbulent channel flow"; *Chem. Engineering Science*; 123; pp. 265 - 282.
14. N.V. Priezhev, S.M. Troian; 2006;"Influence of periodic wall roughness on the slip behaviour at liquid/solid interfaces: molecular-scale simulations versus continuum predictions"; *J. Fluid Mech.*; Cambridge University Press; 554; pp. 25 - 46.
15. S. Jung, M.K. Tiwari, N.V. Doan, D. Poulikakos; 2012;"Mechanism of supercooled droplet freezing on surfaces"; *Macmillan; Nature Communications*; pp. 1 - 8.
16. J. Hallett; 1964;"Experimental studies of the crystallization of supercooled water"; *Journal of Atmospheric Sciences*; 21; pp. 671-682.
17. V.A. Averkov, M.A. Zheltov, V.V. Skvortsov, A.A. Shibkov; 2009;"Morfological instability of interphasial boundary ice-water"; *Phase Transitions, Ordered Conditions and New Materials*; pp. 1- 3.
18. http: // isbu.ac.uk./water/models.html. (25.08.2014).
19. V.A. Tatarchenko; 2010;"Characteristic infrared radiation of the first-order phase transitions and its connection with atmospheric optics"; *Atmospheric and Oceanic Optics*, 23(4); pp. 252-258.
20. A.V. Shavlov; 2005;"The electric potential at the crystallization front of water and solutions. The role of protons and orientation defects"; *Journal Fizicheskoi Himii*; 79(9); pp. 1626-1630; (in Russian).
21. Bo Shi, V.K. Dhir; 2009;"Molecular dynamics simulation of the contact angle of liquids on solid surfaces"; *The Journal of Chem. Phys.*; 034705 (200); pp. 1 - 5.
22. T. Werder, J.H. Walther, R.L. Jaffe, T. Halicioglu, P. Koumoutsakos; 2003;"On the water-carbon interaction for use in molecular dynamics simulations of graphite and carbon nanotubes"; *J. Phys. Chem.*; 107; pp. 1345 - 1352.
23. N. Sedighi, S. Murad, S. Aggarwal; 2010;"Molecular dynamics simulations of nanodroplet spreading on solid surfaces, effect of droplet size"; *Fluid Dyn. Res*; 035501; pp. 1 - 23.
24. I.A. Amelyushkin, A.L. Stasenko; 2015;"Dynamics of molecules in a supercooled water nanoparticle during the ice accretion on the aircraft surface"; *Progress in Flight Physics*; 7; M.: Torus press; pp. 3 - 20.